Giuseppe Cuzzucoli
and Vincenzo Lombardo
Dipartimento di Informatica
Università di Torino
C.so Svizzera 185
10149 Torino, Italy
cuzzucoli@di.unito.it
vincenzo@di.unito.it

A Physical Model of the Classical Guitar, Including the Player's Touch

While stringed instruments have been in use for over 3,000 years, the classical guitar is a relatively young instrument: its proportions and even its technology matured at the end of the 19th century, after a complex evolution of more than three centuries which strongly affected the instrument's architecture and sound quality. The architecture of today's classical guitar is mostly the result of empirical methods. Nevertheless, modern-day luthiers find it convenient to use a more scientific approach in designing and testing their instruments (Garrone 1994). Also, the study of musical instruments has become a topic of complementary disciplines (physics, mathematics, and computer science) that aim at investigating the physical phenomena involved in the mechanics of tone production (Schelleng 1963; Cremer 1984; Meyer 1985).

A particularly obscure aspect is the contribution of the performer's action. Although the importance of the finger-string interaction had already been recognized in the 19th century, only recently have researchers (Taylor 1978; Gilardino 1993) been investigating the relationship between performance technique and sound quality. Understanding these mechanisms would be of great importance. On one hand, it would help performers to be aware of their technique, and to have a deep understanding of what they are doing and why; on the other hand, the physicist could gain a considerable insight into the dynamic behavior of the instrument, by relating the physical qualities of the sound and the instrument mechanisms through some formalization of the playing process.

This article attempts to present a physical model that considers the perspectives of both the musician and the physicist. To this end, we describe a physical model of the *played* classical guitar: we take into account the most significant factors related to the sound-production mechanism, including the performer's touch. Therefore, the model describes the string, the body, the finger action, and the interactions between them. The model's inputs include parameters that can influence the tonal response, such as the body, the string characteristics, and the finger's static and dynamic parameters. In order to simulate the instrument's behavior quantitatively, we have evaluated a set of plausible values for the instrument characteristics and for the finger parameters through a number of simple experiments.

The model is implemented with a modular and efficient architecture that reflects the instrument's architecture: there are modules that implement the string, the resonator, and the finger, respectively, and there are interfaces that implement the string-resonator and the finger-string interactions. The system takes as input the physical parameters of each string, the resonator, and the finger, together with a description of a musical score that includes each note's position on the guitar fret board. The model's final output is a sound file, which helps in evaluating the model's effectiveness. Careful selection of the data structures and algorithms makes possible a simulation time that is comparable to real playing time.

This article is organized as follows. In the next section, we describe the instrument model by addressing its single components (the string and the resonator) and the interaction between them. We then describe the model of the finger and its action on the string. Finally, we discuss the results in terms of the spectra produced by our implementation of the model.

Computer Music Journal, 23:2, pp. 52–69, Summer 1999

The Instrument Model

In this section, we describe the physical models of the relevant components of the guitar. We survey each topic by referring to the literature in the relative area, and illustrate our solution in detail only when it differs from common approaches.

The String

Given the classical equation of the ideal string (Morse 1948; Seto 1971),

$$\mu \frac{\partial^2 y}{\partial t^2} = F_x \frac{\partial^2 y}{\partial x^2} \tag{1}$$

where μ is the mass per unit length and F_x is the string tension, the traveling-wave solution proposed by Morse (1948) and Smith (1992) has computational advantages over the finite-differences method (Chaigne 1992; Chaigne and Askenfelt 1994).

The traveling wave, also known as the D'Alembert solution, is based on the consideration that

$$y(x,t) = y_+(x - ct) + y_-(x + ct) \tag{2}$$

is a solution of Equation 1. The y_+ and y_- terms represent generic waves, traveling on the string in the direction of the positive and negative x (on a guitar, toward the bridge and the nut), respectively. These generic functions y_+ and y_- are completely described once the initial conditions of Equation 1 are fixed.

The data structure that implements this model (Smith 1992) consists of two arrays; each array is associated with one traveling wave. The motion of the waves is implemented by shifting the content of the arrays one position to the left or right at each sampling time. Consequently, the displacement of the string (Y) in each of its spatial samples is the sum of the content of the corresponding elements of the arrays. A specific behavior occurs at the string terminations in the guitar, the nut, and the bridge. If such clamping points are ideal reflectors (i.e., they are infinitely rigid), their displacement will be null at any time: $y(0, t) = y(L, t) = 0$.

In dealing with the real world, one has to augment the previous model by accounting for the following features: (1) string damping, due to the internal friction and to the energy losses in overcoming the air resistance; (2) nonrigid terminations; (3) string-resonator interaction, which makes a vibrating string lose further energy; (4) finite elasticity of the string, which owing to its stiffness makes the wave speed increase with frequency, thus dispersing several waveforms that propagate along the string (*dispersion*); and (5) pitch deviations, owing to the numerical errors introduced by temporal and spatial sampling (*waveguide tuning*).

In the next section, we deal with string damping and nonrigid terminations (including a brief discussion of dispersions); we then describe the solution to tuning problems; finally, we discuss the contribution of the interaction with the resonator to string damping.

String Damping

Damping causes a selective decrement in time of the string motion's amplitude: higher partials decay faster, and as a consequence, the spectral content changes within the course of a single note, with a noticeable influence on the guitar's sound. Introducing damping, Equation 1 becomes

$$\mu \frac{\partial^2 y}{\partial t^2} = F_x \frac{\partial^2 y}{\partial x^2} - r(\omega) \frac{\partial y}{\partial t} \tag{3}$$

where $r(\omega)$ is the damping coefficient, increasing with frequency (Cremer 1984). For small displacements of the string $y(x, t)$, the solution to Equation 3,

$$y(x,t) = e^{\frac{rx}{2\mu c}} y_+(x - ct) + e^{+\frac{rx}{2\mu c}} y_-(x + ct), \tag{4}$$

shows how the amplitude decreases exponentially with time, while the time constant $\tau(\omega)$

$$\tau(\omega) = \frac{2\mu}{r(\omega)} \tag{5}$$

decreases with frequency (De Dayan and Behar 1979).

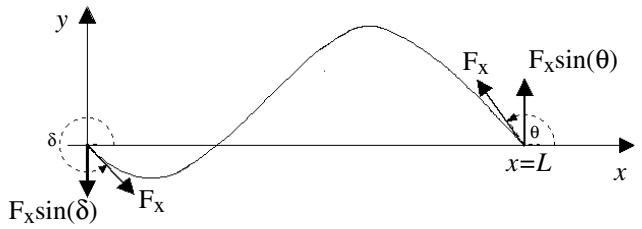

Figure 1. Displacement of the string and forces at the clamping points.

To add damping to the string's digital representation, one has to introduce a damping factor in the quantity which is transferred from one position to the next; or, considering that the digital simulation is linear and time-invariant (Smith 1992), one can commute the loss elements, and lump them at a minimum number of points, possibly one. In particular, we can simulate a lossy string with nonrigid terminations through the single mechanism of applying a proper load to a termination (Smith 1992).

At the nut ($x = 0$), for small angles, the vertical component due to the string tension is

$$F(t) = F_x \frac{\partial y}{\partial t} \tag{6}$$

(see Figure 1). Given the definition of the *mechanical impedance Z*, $F(t) = F_x \frac{\partial y}{\partial t}$, we can relate the displacement at the nut to the mechanical impedance Z_n of the applied load, obtaining the expression of the wave reflected from the nut:

$$y_+ = y_- \frac{R_c - Z_n}{R_c + Z_n}. \tag{7}$$

where $R_c = F_x/c$ represents the string's characteristic resistance, and F_x is the string's tension.

The above relation can be modeled by means of a digital filter whose z-domain transfer function is $H(z)$, such that

$$Y_+(z) = H(z)Y_-(z). \tag{8}$$

The design of the filter must provide: (1) adjustable gain at zero frequency (A_0); (2) adjustable low-pass characteristics (cutoff frequency f_0); and (3) zero or constant *phase delay*, where the phase delay $\tau(\omega)$ introduced by the filter is defined as

$$\tau(\omega) = -\frac{\Theta(\omega)}{\omega}$$

and $\Theta(\omega)$ is the phase response versus frequency (Parks and Burrus 1987).

The first requirement assures that the traveling signal's amplitude decreases in time, provided that the gain is lower than 1; the second requirement assures that the higher partials decay faster than the lower partials; and the third one ensures that the phase relation between the components of the sound is constant, thus avoiding dispersion. Although dispersion plays a role in the heavy strings of the piano (where it can be simulated using an all-pass filter that has an appropriate phase response [e.g., see Smith 1992]), it can be neglected in the case of the guitar, whose strings are highly flexible.

These requirements are fulfilled by a second-order symmetrical finite-impulse-response (FIR) filter, whose z-domain transfer function can be written as

$$H(z) = a_0 + a_1 z^{-1} + a_0 z^{-2} \tag{9}$$

and whose magnitude is

$$\left|H(e^{j\omega T})\right| = 2a_0 \cos(\omega T) + a_1. \tag{10}$$

The phase response of the filter is

$$\Theta(\omega) = \arg\left\{H(e^{j\omega T})\right\} = -\omega T \tag{11}$$

which results in the filter's introducing a constant delay of one sampling period, T.

The transfer function defined by Equation 9 depends on the two parameters a_0 and a_1, which can be adjusted by properly fixing two points in the frequency-versus-magnitude plane. In the current implementation, we select the values A_0 (the gain at zero frequency) and f_0 (the cutoff frequency), such that the gain is $0.7 \times A_0$. The first parameter (A_0) determines the damping of the sound; the second (f_0) determines most of the decay of the higher partials. Figure 2 shows the magnitude of the filter for different values of f_0, ranging between 2 kHz and 10 kHz. Here the gain A_0 is equal for all the curves ($A_0 = 0.95$), while the frequency scale is nor-

malized to the Nyquist frequency.

Once A_0 and f_0 are fixed, one can calculate the values of the parameters:

$$a_0 = \frac{0.3A_0}{2(1-\alpha)};\ a_1 = A_0 - 2a_0;\ \alpha = \cos(2\pi f_0 T). \qquad (12)$$

For each of the six strings and/or for the different notes played on the same string, we have empirically identified proper values for A_0 and f_0 by comparing: (1) the subjectively perceived qualities of the real and the simulated sounds, and (2) the objective decay of the higher partials in the real and simulated sounds.

Finally, from Equation 9, the discrete-time-domain response of the filter is

$$O(m) = a_0 I(m) + a_1 I(m-1) + a_0 I(m-2) \qquad (13)$$

where $O(k)$ and $I(k)$ are respectively the sampled values of the output and input signals at the sampling time k.

It is worth remarking that we can attribute different values of A_0 and f_0 to the same note played on different strings, to simulate the differences in the sound characteristics due to the properties of each string.

Tuning the Waveguides

The waveform resulting from the motion of the waves traveling along the N-element waveguides is periodic, and the frequency of the fundamental is $f_N = f_c/2N$, where f_c is the sampling frequency. At a given sampling frequency, f_c, and for a sound whose fundamental is $f = f_c/2v$,

$$D = 2v - 2N \qquad (14)$$

is the additional delay in the loop necessary for reproducing correctly the pitch of the sound. The problem of introducing a delay D, which is not a multiple of the sampling time, can be solved by designing a numerical algorithm (that is, a digital filter) which must provide constant gain versus frequency, and constant phase delay versus frequency in order not to alter the amplitude and phase relations between the partials of the signals

Figure 2. Magnitude of the second-order symmetric FIR filter (several cut-off frequencies).

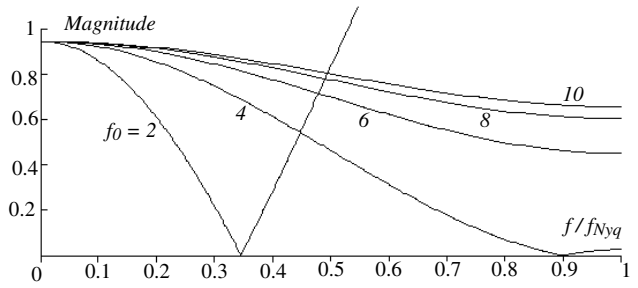

in input to and output from the filter.

A number of techniques have been proposed to design a filter meeting the above requirements (Laakso et al. 1996). A prominent approach is based on the consideration that all-pass filters exhibit constant (unit) gain in the whole frequency range, while the desired phase (or phase-delay) response can be approximated to meet some requirements.

The z-domain transfer function of an Nth-order all-pass filter is

$$H_T(z) = \frac{h_N + h_{N-1}z^{-1} + \ldots + z^{-N}}{1 + h_1 z^{-1} + \ldots + h_N z^{-N}} = z^{-N}\frac{D(z^{-1})}{D(z)} \qquad (15)$$

and the phase delay is

$$\delta = NT - 2\delta_D(\omega) \qquad (16)$$

meaning that the filter introduces a fixed delay of N samples minus a fractional delay equal to twice the delay of the numerator of the transfer function calculated for $z = e^{j\omega T}$.

If the filter must provide constant phase delay, we can apply the Thiran formulation to calculate the filter coefficient in Equation 15. The explicit solution for the coefficients of an Nth-order all-pass filter can be found in the work of Laakso and colleagues (1996). In the case of $N = 2$, we have:

$$h_0 = 1;\ h_1 = -2\frac{\delta - 2}{\delta + 1};\ h_2 = \frac{(\delta - 1)(\delta - 2)}{(\delta + 1)(\delta + 2)} \qquad (17)$$

where δ is the given phase delay that the filter must implement ($1 \le \delta \le 2$)

Figure 3 shows the phase delay introduced by the filter for different values of δ in the frequency range up to the Nyquist frequency; the delay is constant up to $f_{\text{Nyquist}}/2$, and this is sufficient for

Figure 3. Phase-delay response of the second-order Thiran filter.

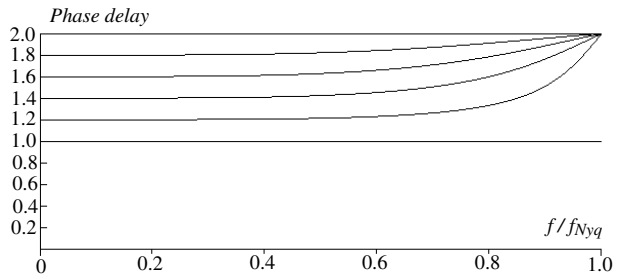

Figure 4. The data structure that implements the two-array model of the plucked string.

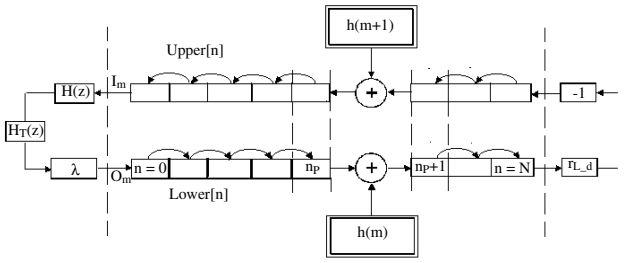

tuning the delay lines (given their length).

The discrete-time-domain response of the second-order Thiran filter is

$$O(m) = h_1\left[I(m-1) - O(m-1)\right] + h_2\left[I(m) - O(m-2)\right] + I(m-2) \quad (18)$$

where $O(k)$ and $I(k)$ are respectively the sampled values of the output and the input signals at the sampling time k. In order to define the filter value correctly, we also have to consider that the second-order symmetric filter that implements the losses (see Equation 9) introduces a delay of one sample. The total delay necessary for reproducing correctly the pitch of a sound (Equation 14) is

$$D = 2v - 2N = \delta + 1 + \lambda \quad (19)$$

where δ is due to the fractional delay filter, and the unit delay is due to the filter of losses. The additional delay λ, which can only take the value 1 or 0, has been introduced to meet the condition $1 \leq \delta \leq 2$. Hence, each note that can be played on the guitar according to the standard tuning is defined, in our model, by the parameters N, δ, and λ.

Figure 4 summarizes the data structure for the complete plucked-string model, including the plucking point, the filters at the nut, and the reflection at the bridge. Only a few points in the structure are relevant to the sound-production mechanism: the nut, in which losses are concentrated (see Equation 8); the plucking point to which the excitation is applied (see the finger-string interaction below); and the bridge, where we have the interaction with the resonator (see the resonator section). Besides these positions, whose displacement is governed by special equations, one can obtain the string's motion simply by shifting one position left and right the arrays associated with the traveling waves. From the implementation viewpoint, we have gotten a relevant computational gain by moving cursors along the vector instead of shifting all the locations' contents.

The Resonator

The bridge is driven into motion by the vibrating string because of the resonator's finite mechanical impedance. At the lowest frequencies, the resonator's response is determined by its basic modes, i.e., by the air resonance (at about 100 Hz) and the main plate resonance (at about 200 Hz) (Jansson 1971). In addition, the higher resonances play an important role in determining the qualities of the sound of the guitar (Meyer 1985). This is because of both the selective amplification on the string partials due to the distribution of the resonant peaks, and the decay rate introduced in the string motion by the body's response. It is extremely difficult to model the body's behavior over the entire audio range. Although we recognize the contribution of the higher modes, currently we take into account only the basic low-frequency resonances; future research will investigate a more adequate model of the resonator behavior.

According to a well-assessed, even if simplified, description of the stringed-instrument resonators (see Schelleng 1963; Agren 1976; Firth 1977; Cremer 1984), we can describe the resonator as an enclosure in which a hole is opened, an arrangement acting as a Helmholtz resonator. The air

Figure 5. Simplified model of the guitar and violin resonator.

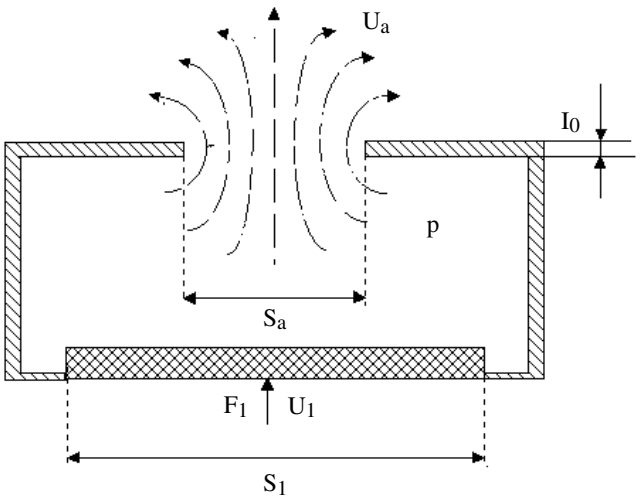

within the cavity and hole is driven into motion by the instrument's resonant table (whose active surface is S_1), to which an external force is applied (see Figure 5). Part of the external force *F(t)* excites the Helmholtz resonator, while the remainder balances the stiffness s_1, the inertia m, and the losses R_p of the plate. With the aid of the electroacoustic analogy, we can represent the system's elements by means of the equivalent electrical network of Figure 6. A similar circuit is discussed by Beranek (1954) to describe the operation of bass-reflex enclosures. In the electroacoustic analogy of Figure 6, the bridge is represented by the circuit input terminals, and the resonator's mechanical impedance $Z(t) = F(t)/U_1(t)$ can be calculated from the equivalent network.

The wave reflected from the bridge is in turn related to *Z(t)*. Introducing the complex poles and zeros of the function, we obtain

$$Z(s) = \frac{F(s)}{U_1(s)} = m\frac{\left(s^t + s\alpha + \omega_1^{\,2}\right)\left(s^2 + s\alpha_2 + \omega_2^{\,2}\right)}{s\left(s^2 + s\alpha_h + \omega_h^{\,2}\right)} \quad (20)$$

where ω_1 and ω_2 are the resonator's natural frequencies, ω_h is the resonant frequency of the Helmholtz resonator, and α_1, α_2, and α_h are damping parameters, each related to the quality factor of the corresponding characteristic frequency as

$$\alpha_j = \frac{2\pi f_j}{Q_j} \qquad Q = \frac{f_j}{\Delta f_j} \ . \quad (21)$$

Figure 6. Electrical network representing the guitar resonator at low frequencies.

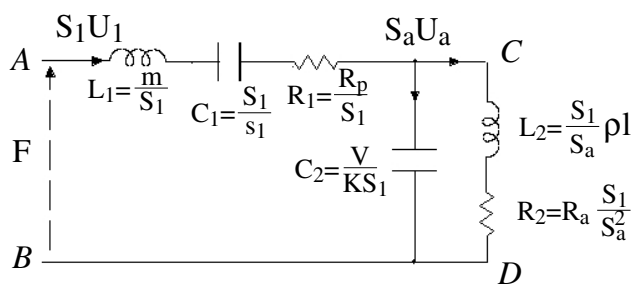

The following values were obtained on a reference instrument by exciting the bridge with a constant-amplitude sinusoidal force and measuring the bridge velocity:

f_1 = 112 Hz	α_1 = 35.2	air resonance	
f_h = 132 Hz	α_h = 38.5	Helmholtz resonance	(22)
f_2 = 212 Hz	α_2 = 80.7	table resonance	
m = 95 g		vibrating mass of the table	

On the same instrument the *mobility*, defined as mob = $20 \log\left(\frac{U_1}{F}\right)\left[\frac{m}{(N \times 5)}\right]$, has been measured and compared with its theoretical value obtained from Equation 20 with the parameters listed in Equation 22. Figure 7 shows that the calculated values agree closely with the measurements. The mobility, a figure normally adopted in investigating the physical properties of vibrating bodies, relates the excitation (normally a constant-amplitude sinusoidal force) to the body's velocity, thus representing how fast the body moves under the excitation of an external force.

Interactions between String and Resonator

Figure 7 demonstrates that Equation 20 accurately represents the resonator's behavior, assuming that its parameters are known. We calculate the reflected wave from the relation

$$y_-(n,m) = y(n,m) - y_+(n,m) \quad (23)$$

resulting from the D'Alembert solution, valid at any sampling point and any sampling time.

From Equation 20, in the Laplace domain, the ratio between the displacement and the force at the bridge is

Figure 7. Mobility of the guitar resonator on the reference instrument and the model.

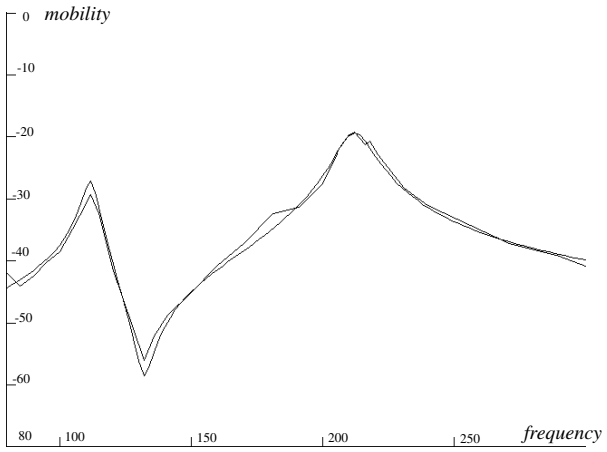

$$\frac{Y(s)}{F(s)} = \frac{1}{m} \frac{\left(s^2 + s \quad \alpha_h + \omega_h^{\,2}\right)}{\left(s^2 + s \quad \alpha_1 + \omega_1^{\,2}\right)\left(s^2 + s \quad \alpha_2 + \omega_2^{\,2}\right)} \tag{24}$$

which can be expressed in the discrete-time domain as

$$\begin{aligned} & w_0 y(N,m) = -w_1 y(N,m-1) - w_2 y(N,m-2) \\ & -w_3 y(N,m-3) - w_4 y(N,m-4) \\ & + \frac{T}{m}\left[d_0 F(m) + d_1 F(m-1) + d_2 F(m-2) + d_3 F(m-3)\right]. \end{aligned} \tag{25}$$

The unconventional *matched-z* transformation rule that has been used here is

$$\begin{aligned} H(s) &= \frac{As + B}{\left(s^2 + s\alpha_2 + \omega_2^{\,2}\right)} = \frac{As + B}{\left(s + x_1\right)^2 + x_2^{\,2}} \\ \rightarrow H(z) &= \frac{AT\left(1 - p_3 z^{-1}\right)}{1 - 2p_1 z^{-1} + p_2 z^{-2}} \; . \end{aligned} \tag{26}$$

The expression of the vertical component of the force at the bridge, valid for small displacements of the string (see Figure 1), is

$$F(t) = -F_x \quad \frac{\partial y}{\partial x}$$

which leads to

$$F(m) = \frac{-F_x}{\Delta}\left[y(N,m) - y(N-1,m)\right]. \tag{27}$$

Figure 8. Bridge displacement for a simulated A open string (110 Hz).

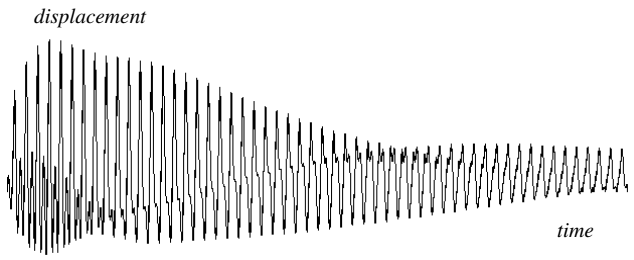

Since Equations 25 and 27 must both be true at the same sampling time, we obtain

$$\begin{aligned} y(N,m) = {} & u_0 y(N,m-1) + u_1 y(N,m-2) \\ & + u_2 y(N,m-3) + u_3 y(N,m-4) \\ & + u_4 y(N-1,m) + u_5 y(N-1,m-1) \\ & + u_6 y(N-1,m-2) + u_7 y(N-1,m-3) \; . \end{aligned} \tag{28}$$

The constant coefficients of Equation 28 are related to known parameters of the string and the resonator; consequently, we can determine both the displacement at the bridge and the amplitude of the reflected wave. Equation 28 can be easily implemented in the context of the data structure previously discussed.

Figure 8 represents the simulated displacement at the bridge for an A2 open string; this note's fundamental frequency (110 Hz) is near to the reference instrument's air resonance (112 Hz). The figure clearly shows the coupling between the first string mode and the air resonance.

Modeling the Sound Pressure

Any musical instrument produces sound-pressure variations in the air that are perceived by the listener. Therefore, the final target of the instrument's physical model is simulation of the sound pressure, which is the physical quantity that allows a comparison between the model's performance and the instrument's tonal characteristics.

Assuming that the radiators can be treated as simple spherical sources, the sound pressure at distance r from the center is

$$SP(s) = -\frac{\gamma}{4\pi r} s U(s) \tag{29}$$

Figure 9. Simulation of the sound pressure for the A open string.

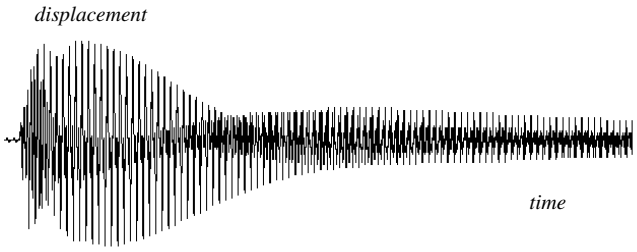

Figure 10. FFT of the simulated sound pressure (a) and measured sound pressure (b) for the A open string.

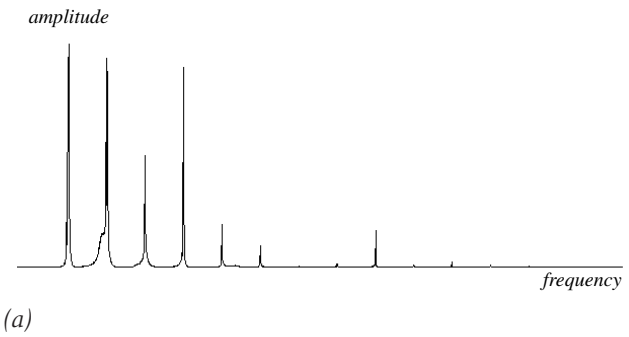

(a)

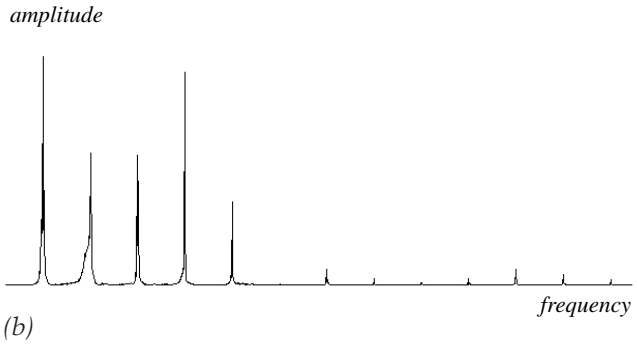

(b)

where $U(s)$ is the volume velocity of the source, and γ is the air density. In the case of the guitar, both the active part of the table and the hole contribute to the sound radiation. From the model of the resonator (see Figure 5), it follows that

$$U(s) = S_1 U_1(s) - S_a U_a(s) . \quad (30)$$

By manipulating the network's equations, it is possible to express the sound pressure as a function of the bridge displacement:

$$SP(s) = -\frac{\gamma}{4\pi r} Y(s) \left[s^2 - \frac{s^2 \omega_h^{\,2}}{s^2 + s\alpha_h + \omega_h^{\,2}} \right] . \quad (31)$$

The discrete-time equivalent representation of Equation 31 can be found again by using the z-transform; the discrete-time representation of the sound pressure is

$$\begin{aligned} SP(m) = {} & w_1 SP(m-1) + w_2 SP(m-2) + w_3 y(N,m) \\ & + w_4 y(N,m-1) + w_5 y(N,m-2) + w_6 y(N,m-3) \\ & + w_7 y(N,m-4) . \end{aligned} \quad (32)$$

Figure 9 shows the simulated sound pressure for an A_2 open string. The magnitude of the fast Fourier transform (FFT) is given in Figure 10, compared with the FFT of the same sound played on a real instrument.

Modeling the Touch and Its Effects on Sound

The importance of touch in relation to the sound's tonal characteristics is well known to all guitarists. Skilled players can obtain fascinating effects from their instruments by controlling the finger's position or its action on the strings. However, only recently have researchers (Taylor 1978; Gilardino 1993) investigated the mechanical aspects of instrumental technique to correlate the obtainable effects to the resources under the player's control. The guitarist can adjust a few basic parameters to produce different sounds: (1) the position of the plucking point along the string; (2) the manner in which the string is excited; (3) the manner in which the string is released; (4) the interaction between the flesh or the nail and the vibrating string before the attack; and (5) the initial displacement of the string, resulting from the plucking force.

While the first and fifth of these parameters are described by only one variable (position or force), the others are complex phases during which the finger-string interaction involves a number of different variables affecting the tone, for example: (1) the duration of the contact, (2) the physical qualities of the body touching the string (in practice flesh, nail, or both), and (3) the amplitude of the force and how it is modulated during the contact.

All of the above considerations lead to the conclusion that the traditional plucked-string representation (the one with a given displacement and zero acceleration in all points before release) is inadequate. A realistic reproduction of the guitar sound can only result from a physical model that describes the player-instrument interaction by taking into account the resources that are under the player's control.

The goal of this section is to model the finger-string interaction by giving emphasis to the control that the performer can act on his finger in terms of the resulting values of selected physical parameters. In our model, the finger is a physical body defined by a mass M_d, a stiffness K_d, and a damping coefficient R_d (cf. Bacon and Bowser 1978).

The force $F(t)$ acting on the string at the plucking point is related to the external force $F_0(t)$ applied by the finger, according to the following expression:

$$F(t) = F_0(t) - (M_d + \mu\Delta)\frac{\partial^2 y}{\partial t^2} - R_d\frac{\partial y}{\partial t} - K_d y \,. \quad (33)$$

Note that we assume for the finger a linear-compression law and a simple fluid-damping coefficient; we claim that the sound quality resulting from the finger-string interaction is mostly related to the way the force is applied or released, and to the values of parameters controlled by the performer. Although the linearity hypothesis does not exactly fit reality, we have empirically verified that it is accurate enough. We develop a notion of control based on the consideration that the performer modifies parameters during the plucking process by loading the string with the hand's weight, playing with the nails rather than the flesh, or smoothing the motion of the string through the flesh's absorbing properties. This reflects a relevant difference between a piano hammer (a typical nonlinear exciter) and a guitarist's finger; with the latter, the possible nonlinearities are only a second-order effect.

When the string is excited at one internal point, the motion of each element of the string results from the combination of four traveling waves (Deb 1972; Hall 1992): (1) the wave that originates at the plucking point and travels toward the nut, (2) the wave that originates at the plucking point and travels toward the bridge, (3) the wave reflected from the nut that travels toward the bridge, and (4) the wave reflected from the bridge that travels toward the nut.

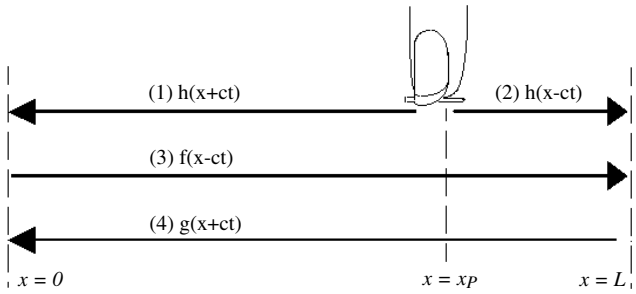

Figure 11. Traveling waves in a plucked string.

Waves 1 and 2 are originated only by action at the excitation point, while waves 3 and 4 are originated by reflections at terminations (see Figure 11).

Given the plucking point x_p, the displacement of each point along the string is given by

$$\begin{aligned} y(x,t) &= f(x-ct) + g(x+ct) + h(x+ct) \quad \text{for } x < x_p \\ y(x,t) &= f(x-ct) + g(x+ct) + h(x-ct) \quad \text{for } x > x_p \\ y(x_p,t) &= f(x_p-ct) + g(x_p+ct) + h(x_p,t) \quad \text{for } x = x_p \end{aligned} \quad (34)$$

which is a particular form of the traveling-wave solution. The excitation wave $h(x,t)$ is related to the force applied to the plucking point $F(t)$; the reflection waves $f(x,t)$ and $g(x,t)$ are related to the impedances of the terminations. The force $F(t)$ is balanced by the internal components of the string tension applied to an element dx that, for small angles, yields the following equilibrium condition:

$$F(t) F_x \left[\left.\frac{\Delta y}{\Delta x}\right|_{x<x_p} - \left.\frac{\Delta y}{\Delta x}\right|_{x>x_p} \right] = F_x D \quad (35)$$

where D is the *difference of increments* at the left and right side of the plucking point. The equation is also valid when the excitation is not concentrated in one single point, but distributed along a segment, provided that the increments are calculated at the extremes of the segment itself. The difference D is calculated considering the waves' propagation along the string and their amplitude increments for $x < x_p$ and $x > x_p$. Finally, the term D of Equation 35 becomes

$$D = \frac{2}{\Delta}\left[h\left(n_p, m\right) - h\left(n_p, m-1\right)\right] + \frac{2}{\Delta} w\left(n_p, m\right) - \frac{1}{\Delta}\left[w\left(n_p, m-1\right) + w\left(n_p, m+1\right)\right] \quad (36)$$

with $w(n,m) = f(n,m) + g(n,m)$.

The amplitudes of $f(n, m)$ and $g(n, m)$ can be evaluated at each point of the string (including the plucking point) by propagating the amplitude of the adjacent sample into the current one or by reflecting the waves at the terminations. Consequently, the string motion is determined when the values $h(n_p, m)$ are known; these values, in turn, depend on the manner in which the excitation mechanism operates on the string.

At the sampling time m and at the plucking point, one possible discrete representation of Equation 33 in terms of finite differences is

$$F\left(m\right) = F_0\left(m\right)\frac{M_d + \mu\Delta}{T^2}\left[y\left(n_p, m+1\right) + y\left(n_p, m-1\right) - 2y\left(n_p, m\right)\right] - \frac{R_d}{2T}\left[y\left(n_p, m+1\right) - y\left(n_p, m-1\right)\right] - K_d y\left(n_p, m\right). \quad (37)$$

After some calculation, we obtain

$$h\left(m+1\right)c_0 = h\left(m-1\right)c_1 + \left[h\left(m\right) + w\left(m\right)\right]c_2 + w\left(m-1\right)c_3 + w\left(m+1\right)c_4 + F_0 c_5 \quad (38)$$

which yields the excitation values at the plucking point, given the finger's physical characteristics and the value of the excitation contributing to the constant parameters.

Given the displacement at the plucking point and the reflection factors at the nut, where losses are consolidated, and at the bridge, where the string interacts with the resonator, the string motion is simulated by shifting the array values (see Figure 4) one position to the left or right.

Modeling the Finger-String Interaction

In this section, we describe the phases of the finger-string interaction, and we evaluate the contribution of the finger parameters to sound quality during each phase. In plucking, the performer first drives the string aside using his or her fingertip, and then releases the string. Moreover, to control the duration of a note or to minimize the noise produced by the string-fingertip contact, the performer has to damp the oscillation of the vibrating string. Summing up, we have identified three phases in guitar-string plucking: excitation, release, and damping. During each phase, the performer is able to control the physical parameters that define the finger; on the basis of a few empirical measures, we have found a range of plausible values for each parameter. Next, we modeled the influence of a parameter on each of the three phases. Finally, we evaluated the model's accuracy by applying FFTs to analyze the harmonic content of both the string displacement and the real spectrum of the sound radiating from the resonator.

In the rest of this section, we first set a range of plausible values for each finger parameter and plucking force to allow a quantitative simulation of the touch. Then, we discuss the influence of the plucking point and the corresponding spectra; finally, we describe the three phases of plucking and the control of finger parameters, also by displaying FFTs that refer to the string displacement. Other data related to touch can be found in the work of Cuzzucoli and Lombardo (1997).

Value Ranges for the Finger Parameters

In this section, we examine the amplitude of the plucking force $F(t)$, the finger's mass M_d, the finger's stiffness K_d, and the finger's damping coefficient R_d.

The amplitude of the plucking force is related to the displacement of the string before its release, and hence to the sound-pressure intensity. One can observe, in normal playing, that the displacement ranges between approximately 1 mm (piano) and 5 mm (forte). A simple experiment, based on applying an increasing weight to a standard E_6 string until a given displacement is reached, has allowed us to conclude that the force applied by the performer ranges between 1–5 N.

The finger's mass M_d cannot be measured directly, but we assume that the performer controls the mass by loading the string with the fingertip, i.e., by relaxing or strengthening the tip while playing. Quantitatively, the mass of the finger lies be-

Figure 12. Damping of the string oscillation for r_d = *2 (a) and* r_d = *8 (b).*

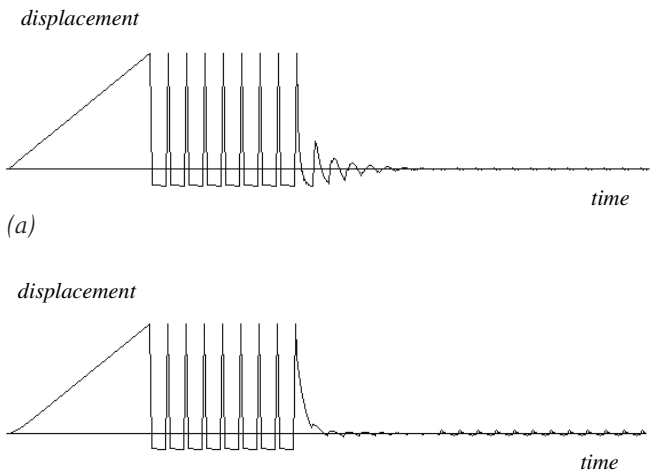

tween that of the electric guitar plectrum (about 200 mg) and that of the piano hammer (about 10 g); we assume that it ranges between 0.5–3 g.

The phalanx touching the string consists of a hard, stiff portion (the nail), which basically draws the string away from its initial position, and an elastic, soft portion (the flesh), which basically damps the string motion by absorbing its energy. By rotating the whole hand from the wrist or bending the tip joint, the guitarist can control both the stiffness and the damping of the finger while touching the string.

The nail's stiffness is probably not far from that of a conventional guitar plectrum, which can be roughly estimated by applying a vertical force to its tip and measuring the vertical displacement. We found that plausible values of the finger's stiffness lie between $K_d = 0$ (when only the flesh draws the string) and $K_d = 3 \times 10^3$ N/m (when the effect of the nail prevails).

The evaluation of the damping coefficient, $r_d = R_d/R_c$, normalized to the string's characteristic resistance, is reported in Figure 12, which shows how the oscillation in the plucking point decays when the string is loaded by the finger (here, $M_d = 0.5$ g, and $K_d = 0$, typical values for mass and stiffness) and no force is applied. The damping coefficient plays a role mainly during transitions between notes on the same string: from this figure, we assume that it normally ranges between 2–5, while only in heavy dampings can it reach 8.

The Position of the Plucking Point

The first parameter influencing sound quality is the position n_p of the plucking point along the string. The spectrum of the displacement for $n_p = N/2$ is shown in Figure 13a; that for $n_p = 3/4\ N$ in Figure 13b, and that for $n_p = 7/8\ N$ is given in Figure 13c. In Figure 13a, the string is plucked midway between the nut and the bridge: only odd partials are present, and in particular, the fundamental stands out over the higher partials. When the plucking point approaches the bridge, in Figures 13b and 13c, the amplitudes of the higher modes increase and the sound becomes more rich and brilliant; note that in Figures 13b and 13c, according to Young's law, the fourth and eighth partials, respectively, are missing.

Here the force acts on just one spatial sample along the string. For $N = 80$ and $L = 65$ cm, the length D of the spatial sample is about 8 mm, corresponding to the real span of the finger-string contact. In principle, one could simulate a wider contact; this would prevent the formation of the higher partials, but the sound would not be substantially influenced (Benade 1976).

String Excitation

In guitar plucking, the string is first driven aside and then released; the sound is unlikely to be affected by the speed at which the finger has approached the string. What does make a difference is the speed with which the nail moves through the string after the first contact or, in other words, the manner in which the string is first driven aside and then released. Certain sounds are produced by a quick impulse of the fingertip on the string (*apoyando*); in other cases, the applied force grows gradually during the attack, giving the string a gentler ride (*tirando*).

In our model, the former action (*apoyando*) is described by applying in Equation 38 a step of

Figure 13. FFT of the displacement for different positions of the plucking point, as a ratio of the distance from the nut to the bridge: 1/2 (a), 3/4 (b), and 7/8 (c).

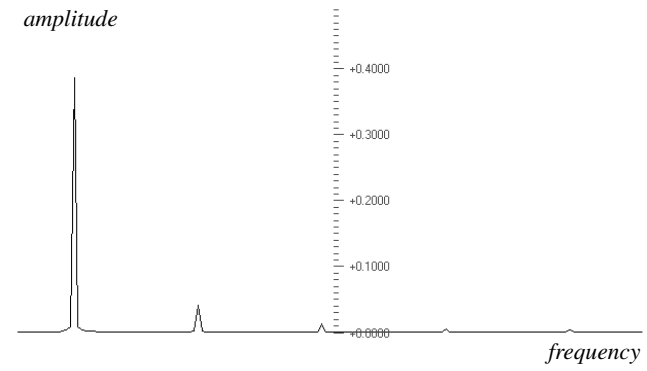

(a)

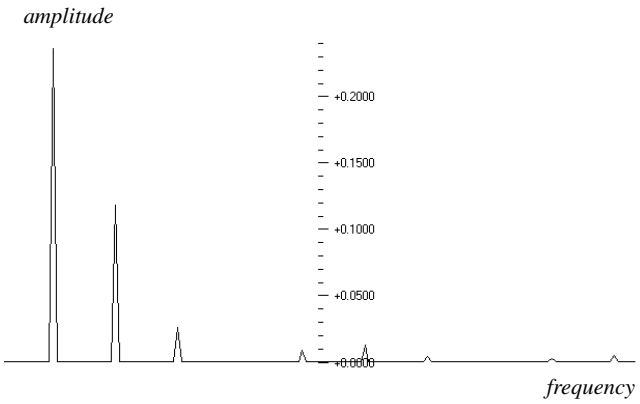

(b)

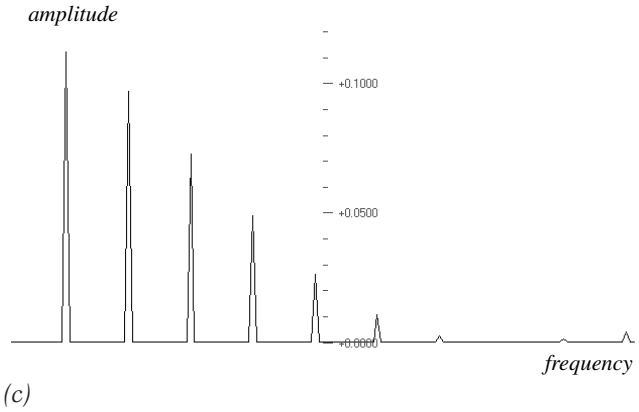

(c)

force $F(t) = F_0$, and maintaining it for a short time before the release. The second action (*tirando*) is described by a linear increase of force during the application time, up to its maximum value F_0:

$$F(t) = F_0 \times \frac{t}{t\_\text{appl}} \ . \qquad (39)$$

Considering that the application time must be short enough to allow execution of a very rapid sequence of notes, we assume that the time for linearly building the force should not exceed 30 msec; in any case, even longer application times have no influence on the sound. (While in principle one can approximate the applied force with more complex laws, we have empirically found that the linear and step approximations are sufficient to represent the basic actions of the player's fingertip on the string.)

When we model the string excitation by assuming that the force is applied stepwise and maintained for only 8 msec (a time which is just enough for the string to reach the final displacement), we obtain the result presented in Figure 14; here the finger parameters are $M_d = 0.5$ g, $r_d = 6$, and $K_d = 10^3$. Figure 15 shows the displacement at the plucking point together with the FFT of its derivative when the force increases linearly during 50 msec.

Finally, in Figure 16, the string is driven stepwise, but the force is maintained for 30 msec before it is realeased. The string comes quickly to its final displacement, but as the finger rests on it, it reacts against the nail and starts oscillating at its natural mode.

The damping coefficient r_d tends to smooth transient oscillations that can occur during plucking, mainly when the force is applied stepwise. The higher the mass, the higher the reaction of the string on the tip, provided the damping coefficient is low. In Figure 17, we show the displacement of the string at the plucking point for $r_d = 6$ (a relatively high value of damping) and for two values of the mass, $M_d = 0.5$ g and $M_d = 3$ g, respectively. The waveforms are quite similar, so we can expect a similar distribution in the string modes' amplitudes.

The situation appears to be different when the damping coefficient is low ($r_d = 1$). In Figure 18, we can see a noticeable reaction of the string against the fingertip when the mass is high (which likely

*Figure 14. Displacement (a) and FFT of the string velocity (b) at the plucking point, for a stepwise application of the force (*t_appl. *= 8 msec).*

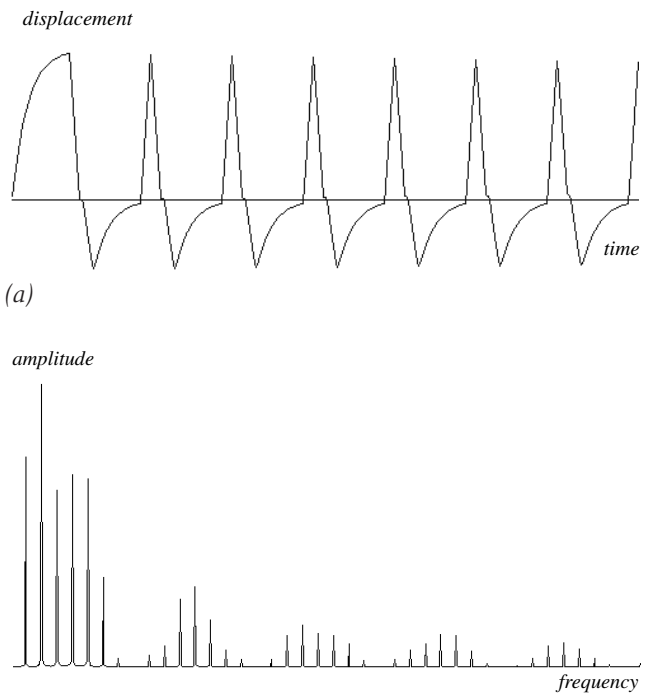

Figure 15. Displacement (a) and FFT of the string velocity (b) at the plucking point, for t_appl. *= 50 msec.*

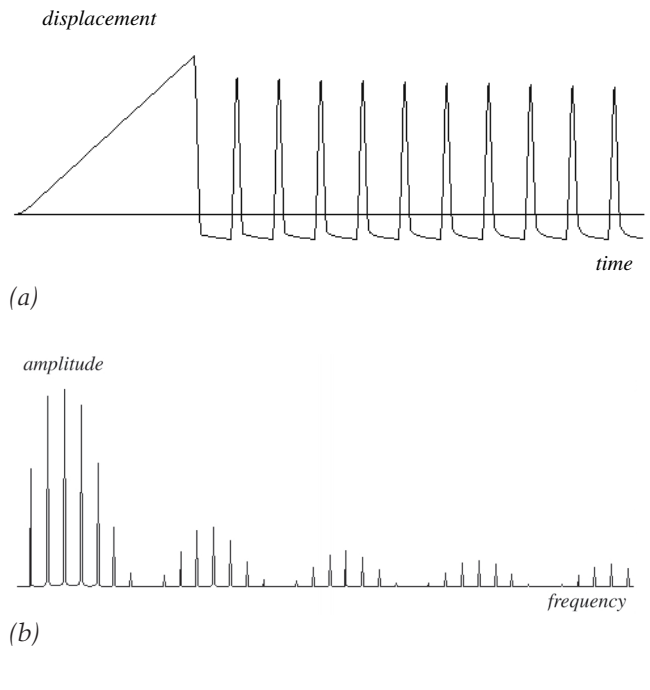

*Figure 16. Displacement (a) and FFT (b) for a stepwise application of the force (*t_appl. *= 30 msec).*

corresponds to a more firm action by the performer).

The influence of the mass M_d is lower when the force is applied linearly, probably because all transients due to the string-to-fingertip interaction during the excitation have time to extinguish before the string is released. The distribution of partials represented in Figure 19 shows that when the excitation is linear the fundamental prevails over the higher partials.

In summary, when the force increases linearly during the excitation time, the fingertip parameters have little influence on the sound, because it does not matter how the string comes to its final displacement, provided the excitation is long enough for the transients to die away. If the string is pulsed, the fingertip-string interaction is more evident when the mass is high. Moreover, the lower the damping coefficient, the higher the string reaction. In the former situation (linear application), the fundamental prevails; in the latter (stepwise application), the higher partials prevail.

Figure 17. Displacement with two values of the tip's mass, for $r_d = 6$*:* $M_d = 0.5$ *g (a) and* $M_d = 3$ *g (b).*

Figure 18. Displacement with two values of the tip's mass, for $r_d = 1$*:* $M_d = 0.5$ *g (a) and* $M_d = 3$ *g (b).*

Figure 19. FFT for $r_d = 1$ *in the case of step (a) or linear (b) application of the force.*

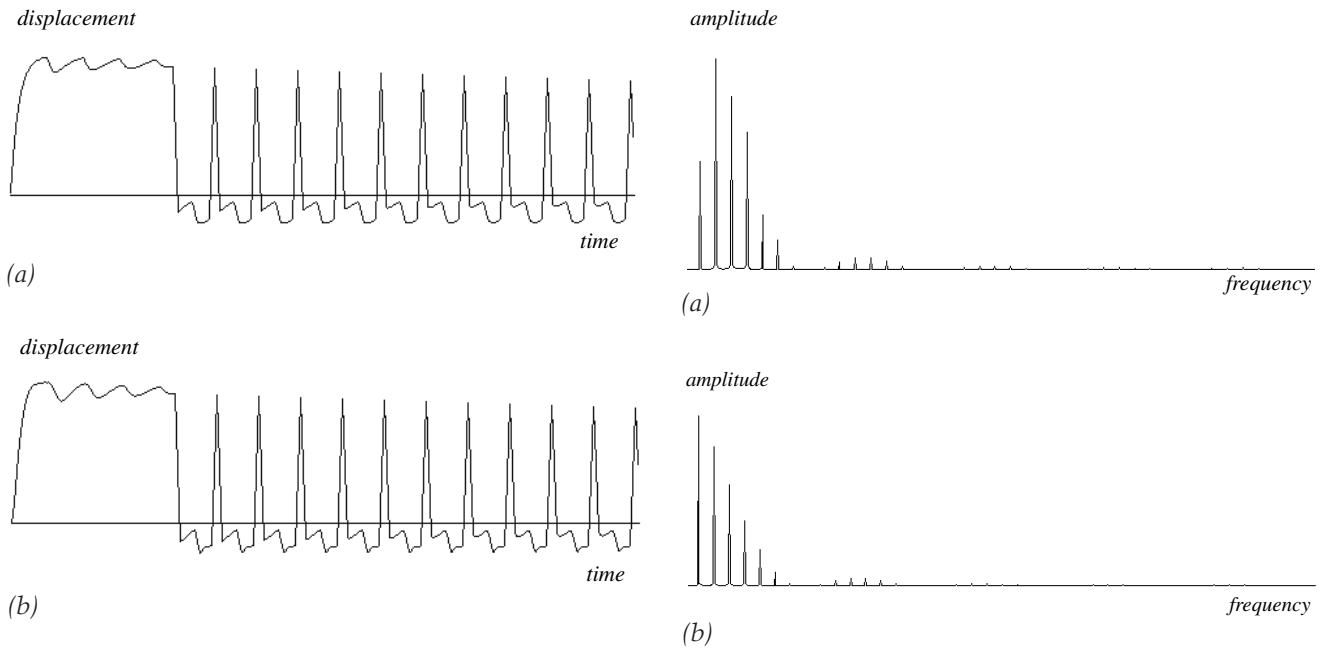

Figure 18

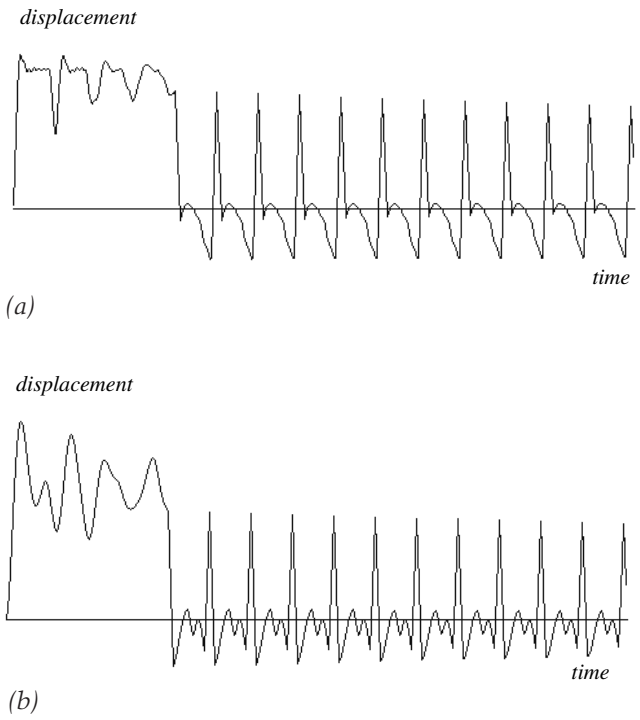

String Release

When the force that displaces the string is suddenly removed, the string tension, no longer balanced by the external force, acts at the plucking point and drives all the points between the terminations into motion. The sudden jerking of the string into motion and the consequent and sudden variation of displacement excites the higher modes. Conversely, these modes can be suppressed by releasing the string gradually. The guitarist controls the release by presenting the tip in such a way that the string can slide over the flesh (or the nail) for a certain time before leaving it. During this release time, the force that was keeping the string in place is removed gradually, but the finger is still in contact with the string and interacts with it by smoothing its initial motion. This interaction is consequently dominated not only by the time during which the string is released, but also by the physical properties of the tip.

To transfer these ideas to our model, we make the assumption that the force is removed gradually during the release:

Figure 20. FFT of the of the string velocity at the plucking point in two release-time conditions: instantaneous release (a) and gradual release (b).

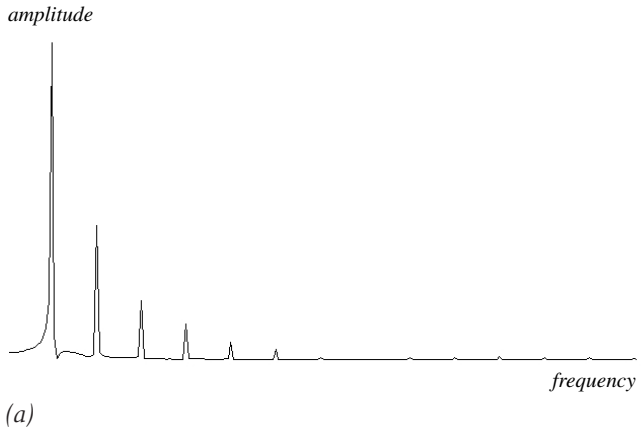

(a)

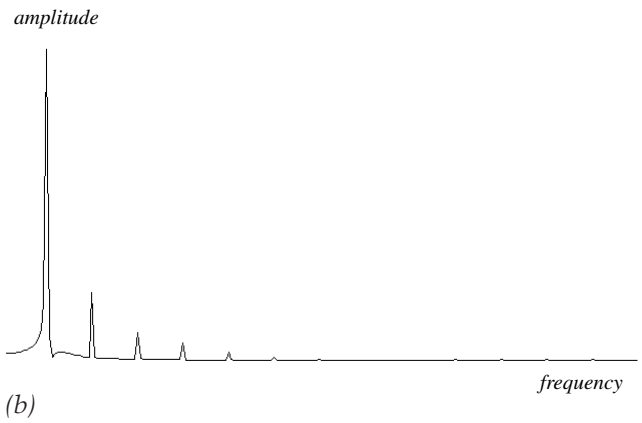

(b)

$$F(t) = F_{\text{Max}} \times \left(\frac{t - t\_\text{appl}}{t\_\text{rel}} \right). \qquad (40)$$

We also assume that the string can slide over the tip for a period not longer than a half-cycle of its motion (to avoid big energy losses): this limits the release time to a few milliseconds. This description of the release phase allows us to introduce a new set of mechanical parameters for the fingertip, M_{d_r}, K_{d_r}, and r_{d_r}, respectively, which again one can correlate to the instrumental technique. The M_{d_r} parameter is lower when a more relaxed action occurs; K_{d_r} is higher when the release is performed mainly by using the nails; and the normalized damping coefficient r_{d_r} is associated with the flesh's absorbing properties during release. With reference to Equation 38, we calculate a new set of constants from these new fingertip parameters.

Figure 21. Release in two different stiffness conditions: $K_{d\_r} = 1 \times 10^3$ N/m (a), and $K_{d\_r} = 5 \times 10^3$ N/m (b).

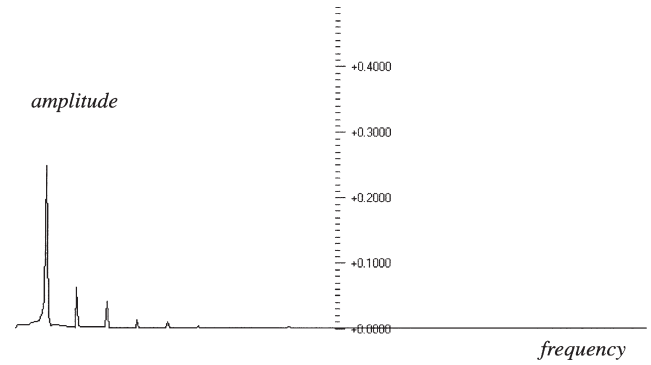

(a)

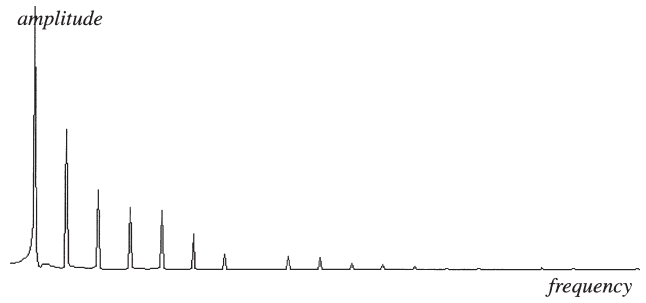

(b)

To check the consistency of the model's results with the ideas discussed before, we simulate some typical conditions of release duration, tip stiffness K_{d_r}, and damping coefficient r_{d_r}. In Figure 20a, the release is instantaneous; in Figure 20b, the force is removed gradually. One can note that in Figure 20b the amplitude of the higher modes is lower than in Figure 20a.

Regarding tip stiffness, in Figure 21a, $K_{d\_r} = 1 \times 10^3$ N/m; in Figure 21b, $K_{d\_r} = 5 \times 10^3$ N/m. Clearly in Figure 21b, where we simulate the intervention of the nail in release, the higher string modes are more important than in Figure 21a. It is well known that the use of the nails gives the sound a particularly clear—somehow metallic—character.

Finally, regarding the damping coefficient, Figure 22a shows the distribution of harmonics for $r_{d\_r} = 0$ (no damping at all); in Figure 22b, $r_{d\_r} = 3$, a relatively high damping coefficient.

Figure 22. Influence of damping during release: $r_{d\_r} = 0$, *or no damping (a), and* $r_{d\_r} = 3$, *or high damping (b).*

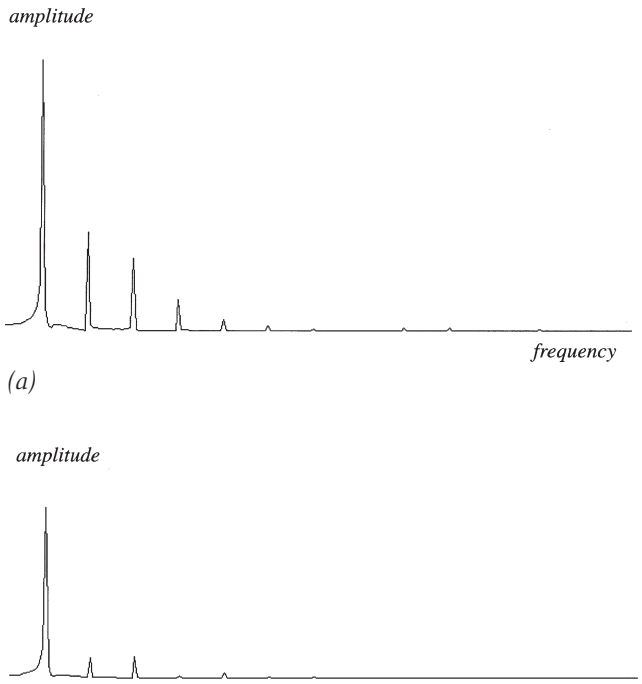

Figure 23. Damping the string with two different damping coefficients: $r = 4$ *(a), and* $r = 1$ *(b).*

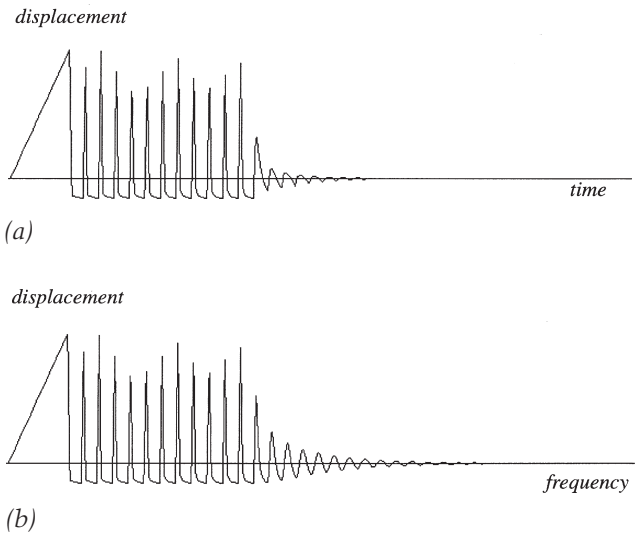

The higher the damping and the longer the release time, the lower the amplitude of high string modes. By working with very long times or very high dampings, one can simulate particular effects like pizzicato, a technique in which the vibration of the string is strongly damped and the reverberation of the note is consequently short. In summary, by modelling different situations that can occur during release, we found that: (1) a sudden release excites higher string modes, while the fundamental stands out otherwise; (2) a high stiffness value aids the excitation of higher modes; and (3) conversely, the damping coefficient prevents the excitation of higher modes.

String Damping

The last aspect of touch that we deal with is string damping. String damping occurs when the performer has to extinguish the string's oscillation, to control the duration of a note or to minimize the noise produced by the contact of the string with the fingertip before plucking it again. String damping is effected by touching the string with the flesh, without exerting any force on the string, that is, without loading the string with the weight of the hand. To model this action, we set all the finger parameters, except the normalized damping coefficient, to zero in the perturbation function. During this phase, the motion of the string is governed by

$$\mu dx \frac{\partial^2 y}{\partial t^2} = F_x dx \frac{\partial^2 y}{\partial t^2} - R \frac{\partial y}{\partial t} \qquad (41)$$

in which R is the damping coefficient. As for the case of exciting the string, the action of the fingertip on the string produces an excitation wave that travels from the plucking point to the terminations, and can be calculated from Equation 38:

$$h(m+1) = h(m) + \frac{\alpha}{1+\alpha}\left[w(m-1) - w(m+1)\right], \qquad (42)$$

where $\alpha = \frac{RT}{2\mu\Delta}$, and R is the damping-coefficient value selected for the damping phase. In Figures 23a and 23b, one can see the effect on the string vibration for two normalized damping coefficients, respectively $r = 4$ and $r = 1$; once again $r = R/R_c$, where R_c is the string impedance. In Figure 23a, the damp-

Figure 24. String damping between two notes.

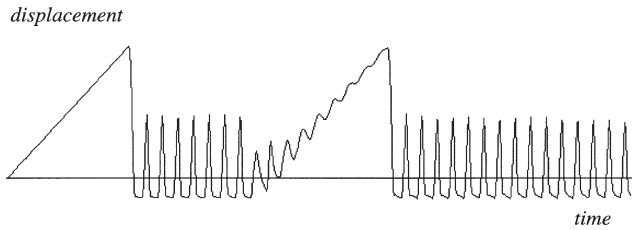

ing effect is higher, so that the oscillation's amplitude tends to decrease faster than in Figure 23b; notice that the envelope of the peaks decays exponentially, the time constant being higher in Figure 23b than in Figure 23a.

The string damping is fundamental in simulating consecutive notes played on the same string. In Figure 24, we show the effect of the string damping between two notes (which have the same pitch); here the attack is linear (M_d = 0.5 g, r_d = 1, K_d = 0) and the damping time is relatively long (10 msec). The damping of the string in contact with the fingertip is concentrated at the plucking point, while elsewhere along the string there are waves, not yet damped, still moving in the direction of the terminations. After reflection, these waves arrive at the plucking point, where they can have an influence on the motion.

In Figure 24, the motion of the string during the attack is a combination of the previous not-yet-extinguished oscillation, with the displacement driven by the plucking force. The string displacement is the same for both notes, and the influence on the sound is not very relevant (except for the audible rattle due to the residual oscillation during the second attack). But, if the attack is short, the residual oscillation (due to incomplete damping) can modify the string displacement at the second note, and consequently, does have a noticeable effect on the sound. This effect, which is easily reproduced and explained with the aid of the model, is commonly experienced by guitarists.

Conclusions

This article has presented a physical model of the played classical guitar. The model covers the relevant aspects of the tone-production mechanisms, related to both the instrument's physics and the performer's action. The latter aspect is particularly important, because as far as we know, there are no other models that attempt to provide a simulation, in physical terms, of the player's technique.

The instrument model includes both the string and the resonator. The string model relies on the popular digital waveguide method (Smith 1992), which leads to a fast and precise simulation algorithm; the model of the resonator is a simplified description that acts as a Helmholtz resonator. Even with severe limitations, this resonator model is a distinctive feature of our totally physical approach, where the use of filters is restricted to the simulation of losses and tuning (the latter due to the accumulation of error caused by digital sampling).

One original contribution of this work concerns the interaction between the string and the resonator: the computation of the transfer function occurs in the z-plane after the application of an unconventional transformation rule; the computation of the wave reflected at the bridge relies on the relation between the bridge displacement and the external force (the vertical component). These methods are general, and can be extended to other stringed instruments.

The simulation of the player's action on the string involves a model of the finger, based on a few physical parameters, and its interaction with the string model. In particular, we have computed the excitation wave as a result of the finger's action on the string. The dynamics of the string displacement depend on the finger parameters and the details of the finger-string interaction. We have identified and modeled three different temporal phases of the player's action on the string (excitation, release, and damping), and we have evaluated the results of the simulations in terms of the spectral components of the sounds. The findings, which are basically in agreement with common musical experience, can help in explaining physically the variety of fascinating sounds that a skilled guitarist can obtain. However, this is only a preliminary study of the nature of touch and its effects on tone production.

Many aspects of this work can be improved. The string model should include the physics of the stiffness, and not only its global effect on the string be-

havior; and the resonator model, though well assessed, is not sufficient to take care of the higher resonances, which play an important role in a realistic tone-production mechanism. Finally, as stated above, the model of the performer's touch must be considered only as a preliminary insight into a complex and only partially investigated problem.

References

Agren, C. H. 1976. "Experimental Findings Concerning Cavity-Assisted Resonances in Stringed Instruments with a Soundpost." *Physica Scripta* 14:179–186.

Bacon, R. A., and J. M. Bowser. 1978. "A Discrete Model of a Struck String." *Acustica* 41:21–27.

Benade, A. H. 1976. *Fundamentals of Musical Acoustics*. Oxford University Press.

Beranek, L. 1954. *Acoustics*. New York: McGraw-Hill.

Chaigne, A. 1992. "On the Use of Finite Differences for Musical Synthesis." *Journal Acoustique* 5:181–211.

Chaigne, A., and A. Askenfelt. 1994. "Numerical Simulation of Piano Strings." *Journal of Acoustical Society of America* 95:1112–1118.

Cremer, L. 1984. *The Physics of the Violin*. Cambridge, Massachusetts: MIT Press.

Cuzzucoli, G., and V. Lombardo. 1997. "Physical Model of the Plucking Process in the Classical Guitar." *Proceedings of the 1997 International Computer Music Conference*. San Francisco: International Computer Music Association, pp. 172–179.

Deb, K. K. 1972. "Dynamics of the Pianoforte String and Hammer." *Journal of Sound Vibration* 20:1–7.

De Dayan, H. G., and A. Behar. 1979. "The Quality of Strings for Guitars: An Experimental Study." *Journal of Sound Vibration* 64:421–431.

Firth, I. M. 1977. "Physics of the Guitar at the Helmholtz and First Top Plate Resonances." *Journal of Acoustical Society of America* 61:588–593.

Garrone, M. 1994. *La Costruzione della Chitarra Classica*. Ancona, Italy: Berben.

Gilardino, A. 1993. *Nuovo Trattato di Tecnica Chitarristica*. Ancona, Italy: Berben.

Hall, D. 1992. "Piano String Excitation VI. Nonlinear Modeling." *Journal of the Acoustical Society of America* 92:95–105.

Jansson, E. 1971. "A Study of Acoustical and Hologram Interferometric Measurements of the Top Plate Vibrations of a Guitar." *Acustica* 25:95–100.

Laakso, T, V. Vlimki, M. Karjalainen, and U. Laine. 1996 "Splitting the Unit Delay." *IEEE Signal Processing Magazine* 13:30–60.

Meyer, J. 1985. *Akustik der Gitarre in Einzeldarstellungen.* Frankfurt: Verlag E. Bochinkski.

Morse, P. M. 1948. *Vibration and Sound*. New York: McGraw-Hill.

Parks, T. W., and C. S. Burrus. 1987. *Digital Filter Design*. New York: Wiley.

Schelleng, J. 1963. " The Violin as a Circuit." *Journal of the Acoustical Society of America* 35:326–338.

Seto, W. 1971. *Acoustics*. New York: McGraw-Hill.

Smith, J. O. 1992. "Physical Modelling Using Digital Waveguides." *Computer Music Journal* 16(4):74–91.

Taylor, J. 1978. *Tone Production on the Classical Guitar*. London: Musical New Services.